PAPER • OPEN ACCESS

A study of quantum Hall devices with different working magnetic fields for primary resistance metrology

OPEN ACCESS
IOP Publishing

Measurement Science and Technology

Meas. Sci. Technol. **28** (2017) 075005 (4pp)

https://doi.org/10.1088/1361-6501/aa6709

A study of quantum Hall devices with different working magnetic fields for primary resistance metrology

Xueshen Wang, Qing Zhong, Jinjin Li, Yuan Zhong and Mengke Zhao

Key Laboratory for the Electrical Quantum Standard of AQSIQ, National Institute of Metrology, 18 Bei San Huan Dong Lu, Beijing 100013, People's Republic of China

E-mail: jinjinli@nim.ac.cn

Received 22 January 2017, revised 9 March 2017
Accepted for publication 15 March 2017
Published 13 June 2017

Abstract

Two kinds of quantum Hall devices with different working magnetic fields are fabricated and compared with the LEP (Laboratoires d'Electronique Philips) device, which is currently used in the primary resistance standard system of the National Institute of Metrology (NIM) of China. The comparison is made by calibrating the same 1 Ω standard resistor made by the National Measurement Laboratory of Australia using a Tinsley 100 Ω resistor as the intermediate standard and a cryogenic current comparator. The calibrated values from the NIM device with high working magnetic field and those from the LEP device agreed to within -0.69×10^{-9} with an uncertainty of 4.9×10^{-9}. The values from the NIM device with low working magnetic field and those from BIPM-2 agreed to within 2.5×10^{-9} with an uncertainty of 7.1×10^{-9}.

Keywords: quantum Hall effect, resistance standards, heterojunction, cryogenic current comparator

(Some figures may appear in colour only in the online journal)

1. Introduction

The quantum Hall effect (QHE) provides a metrological resistance standard in terms of the Planck constant h and elementary charge e [1]. The QHE relies on a 2D electron gas (2DEG), which can be realized in several material systems such as Si-MOSFETs, GaAs/Al$_x$Ga$_{1-x}$As heterostructures or graphene. The GaAs/Al$_x$Ga$_{1-x}$As-based device is the one most used for resistance standard applications [2]. Practical metrological measurements are performed at the $i = 2$ plateau, the quantized resistance at which a filling factor of 2 equals half of $R_{\text{K-90}}$, which is 12 906.4035 Ω [3–10].

In the National Institute of Metrology (NIM) of China, the currently used quantum Hall devices for the resistance standard system (known as BIPM-2) are made by Laboratoires d'Electronique Philips (LEP) and supplied by BIPM (the International Bureau of Weights and Measures) [11, 12]. NIM has recently started to develop its own devices for the quantum Hall resistance standard [13–15]. In this paper we report the development of two devices for the quantum Hall standard: one has a high working magnetic field above 10 T (NIM-1), and the other has a low working magnetic field below 7 T (NIM-2). Devices operating at a low magnetic field could be used as an economic metrological resistance system, having a small magnet which uses less liquid helium [16]. NIM-1, NIM-2 and BIPM-2 are compared by calibrating the same NML 1 Ω standard resistor using a Tinsley 100 Ω resistor as the intermediate standard and a cryogenic current comparator (CCC) as the method of measurement.

2. Device fabrication

The GaAs/Al$_x$Ga$_{1-x}$As 2DEG wafers used for the quantized Hall devices were grown on a three-inch GaAs substrate by molecule beam epitaxy (MBE). The detailed layer structures

Table 1. Layer structures of the heterojunction.

Layers	Thickness (nm) NIM-1	NIM-2
GaAs:Si 1.4×10^{18} cm^{-3}	10	10
$Al_{0.28}Ga_{1-0.28}As$:Si 1.4×10^{18} cm^{-3}	50	50
$Al_{0.28}Ga_{1-0.28}As$ (spacer)	10	14
GaAs	500	500
GaAs/$Al_{0.28}Ga_{1-0.28}As$ 10×	15/185	15/185
GaAs buffer	200	200
GaAs substrate	3 inch	3 inch

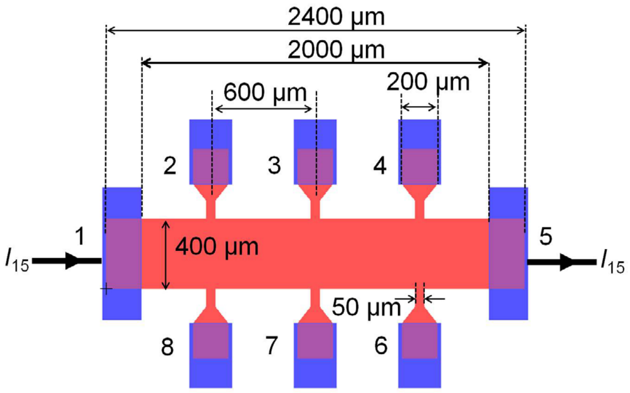

Figure 1. Structure of the NIM-1 and NIM-2 devices: the pink and blue layers represent the Hall bar and the contacts respectively. The scales of the structure are labeled: 1 and 5 are the current pads; 2–4 and 6–8 are the voltage pads.

of the NIM-1 and NIM-2 wafers are given in table 1. The heterojunction was modulation doped. The central magnetic flux density B_{2c} for the $i = 2$ plateau, which is proportional to the carrier concentration of the 2DEG, was tuned by changing the thickness of the spacer layer.

Figure 1 shows the structure of the quantum Hall resistance (QHR) device. The 2400 μm × 400 μm Hall bar mesa (pink layer) was defined by a standard photolithography process followed by wet chemical etching using a solution of H_3PO_4, H_2O_2 and deionized water with a volume ratio of 2:8:90. The Au(1072 nm)/Ge(528 nm)/Ni(400 nm) contacts (blue layer) were formed by sequential e-beam deposition and a lift-off process, and then Ohmic contacts were achieved by rapid thermal annealing at 370 °C for 120 s and 430 °C for 50 s in a N_2/H_2 gas atmosphere. The portion of the contact pads outside the Hall bar was used for Au wire bonding to ensure that the heterojunction was not affected during the wire bonding process. No SiN_x protection layer was grown on top of the QH mesa since it would introduce stress on the 2DEG layer and possibly result in changes in the electrical properties. The fabricated devices were mounted on home-made non-magnetic TO-8 ceramic holders. The inset of figure 2 shows a photograph of a prepared QHR device.

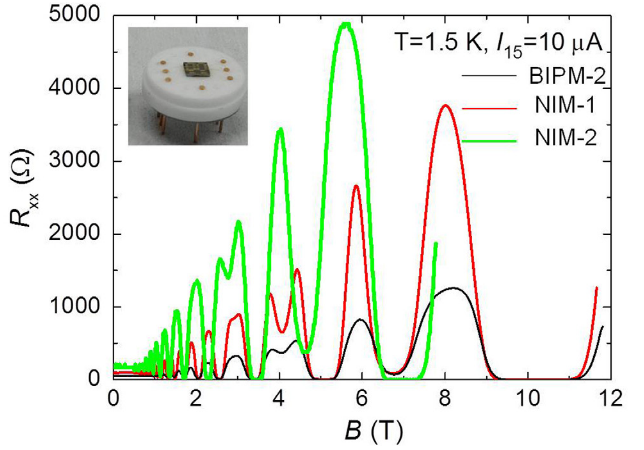

Figure 2. Longitudinal resistance R_{xx} of the devices BIPM-2, NIM-1 and NIM-2 as a function of applied magnetic flux density at 1.5 K with bias current $I_{15} = 10$ μA. The inset shows a prepared QH device mounted on the NIM-made TO-8 carrier, which is composed of 8 BeCu pins, a ceramic plate and a Teflon cap.

3. Measurement

The BIPM-2, NIM-1 and NIM-2 devices were then characterized in the NIM QH resistance standard system which consists of an Oxford magnet (16 T), a high-accuracy current source, an EM N11 voltage meter and the CCC. The devices were slowly cooled to 1.5 K. Three important device parameters, namely central magnetic flux density B_{2c}, residual longitudinal resistance R_{xx} at B_{2c}, and contact resistance R_c at the $i = 2$ plateau, were measured.

The longitudinal resistance R_{xx} is equal to V_{xx}/I_{15}, where V_{xx} can be V_{24} or V_{86} obtained from the EM N11 voltage meter, and I_{15} is the current flowing through the device. The central magnetic flux density B_{2c} at the $i = 2$ plateau is determined by sweeping the magnetic flux density B and measuring the longitudinal resistance R_{xx}; the typical bias current I_{15} used in this process is 10 μA. Once B_{2c} is determined, we set the magnetic field to B_{2c} and measure the residual longitudinal resistance at B_{2c}. In this process I_{15} is set to 38 μA. The contact resistance R_c is measured using a three-terminal technique. The width of the $i = 2$ plateau ΔB_2, mobility μ and carrier concentration n of the devices were calculated from the R_{xx}–B curves. The characterized parameters of the three devices are listed in table 2.

Figure 2 shows the R_{xx} of the devices BIPM-2, NIM-1 and NIM-2 as a function of B at 1.5 K with a 10 μA bias current. The B_{2c} of NIM-1, which is 10.24 T, is close to that of BIPM-2 due to the similar carrier concentration. The magnetic field width at the $i = 2$ plateau ΔB_2 is about 2 T for BIPM-2 and NIM-1. The mobility of NIM-1 is lower than that of BIPM-2. NIM-1 is designed to replace BIPM-2 as the standard device for the NIM QHR standard system.

NIM-2 is designed specifically for a low magnetic field resistance standard system. The B_{2c} of NIM-2 is only 6.88 T and the corresponding carrier concentration is as low as 3.32×10^{15} m^{-2}. ΔB_2 is only about 0.89 T for NIM-2 because of the closer Landau levels due to the low carrier concentration; the mobility is 33.2 T^{-1}.

Table 2. Characterization of the BIPM-2, NIM-1, and NIM-2 devices at 1.5 K and the $i = 2$ plateau.

Devices	$\boldsymbol{B}_{2c}$ (T)	$\Delta\boldsymbol{B}_2$ (T)	μ (T^{-1})	n (10^{15} m^{-2})	$\boldsymbol{R}_{xx}$ at $\boldsymbol{B}_{2c}$ (mΩ) By N11	$\boldsymbol{R}_c$ (Ω)
NIM-1	10.24	1.99	40.4	4.94	0.63	1.6
BIPM-2	10.25	1.99	56.4	4.95	0.63	1.3
NIM-2	6.88	0.89	33.2	3.32	0.40	2.0

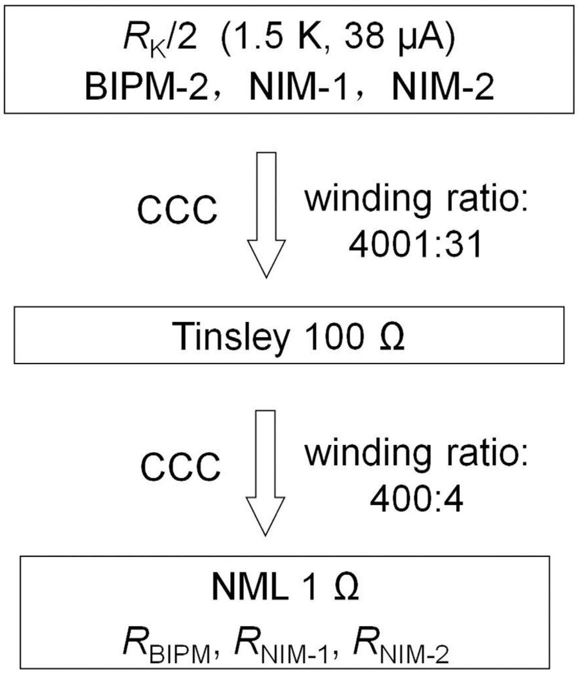

Figure 3. Calibrating an NML 1 Ω standard resistor using a CCC with a Tinsley 100 Ω transfer resistor as the intermediate standard.

For all three devices, the longitudinal resistance R_{xx} at B_{2c} is less than 0.63 mΩ ($V_{xx} < 0.02$ μV) which is close to the measurement limit of the EM N11 voltage meter, as affected by the lab conditions. R_c is measured using a three-wire method at B_{2c}, so both the wire resistance and R_{xx} are included. The R_c values of the three devices are all <2 Ω, which is small enough for metrological measurements [17, 18]. R_{xx} and R_c show that the NIM devices have been completely quantized and can be used as the standard devices in the QHR standard system.

We have compared the devices BIPM-2, NIM-1 and NIM-2 by undertaking a calibration measurement of an NML 1 Ω standard resistor. Figure 3 shows the calibration procedure. First we used these three QH devices to calibrate a Tinsley 100 Ω transfer resistor using a CCC with a winding ratio of 4001:31 and a 0.5 V bridge voltage. The QH voltage V_{xy} was achieved from voltage pads 3 and 7, and $I_{15} = 38$ μA. Then we used the calibrated Tinsley 100 Ω resistor to calibrate the NML 1 Ω standard resistor using the CCC with a winding ratio of 400:4 and a 0.05 V bridge voltage. The calibration values of the NML 1 Ω standard resistor by BIPM-2, NIM-1 and NIM-2 are labeled as R_{BIPM} and R_{NIM} ($R_{NIM\text{-}1}$, $R_{NIM\text{-}2}$). Both the Tinsley 100 Ω and 1 Ω resistors were kept in a 293 K oil bath.

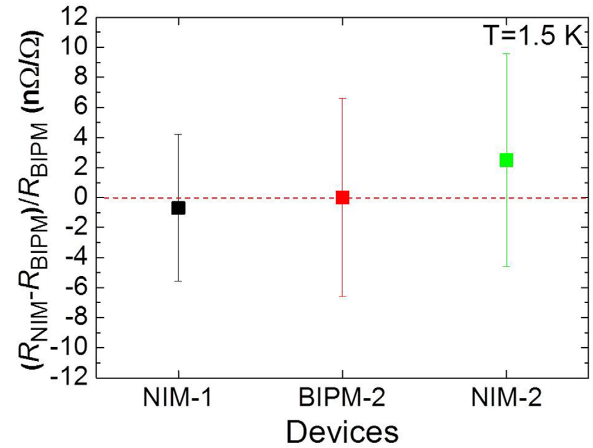

Figure 4. Relative difference of the calibration results of R_{BIPM} and R_{NIM} ($R_{NIM\text{-}1}$, $R_{NIM\text{-}2}$).

The calibration results are shown in figure 4. The vertical axis represents the relative difference of the calibration values, expressed as $(R_{NIM} - R_{BIPM})/R_{BIPM}$. For NIM-1 and BIPM-2, the calibration values agreed to within -0.69×10^{-9}; for NIM-2 and BIPM-2, they agreed to within 2.5×10^{-9}. For this calibration measurement, the combined standard uncertainty u_c includes the uncertainty u_1 of the Tinsley 100 Ω resistor, the uncertainty u_2 of the NML 1 Ω resistor and the system uncertainty u_3, and $u_c = (u_1 \times u_1 + u_2 \times u_2 + u_3 \times u_3)^{1/2}$. u_3 is 0.24×10^{-9} [19], and u_1 is 2.5×10^{-9}, 0.6×10^{-9} and 1.7×10^{-9} for the values from BIPM-2, NIM-1 and NIM-2, respectively. u_2 is 6.1×10^{-9}, 4.9×10^{-9} and 6.9×10^{-9} for the corresponding values from BIPM-2, NIM-1 and NIM-2. So u_c for $R_{BIPM\text{-}2}$, $R_{NIM\text{-}1}$ and $R_{NIM\text{-}2}$ is 6.6×10^{-9}, 4.9×10^{-9} and 7.1×10^{-9}, respectively. These values are a little large for the three devices because of the two-stage calibration chain.

4. Conclusions

Single quantum Hall devices with high (above 10 T, NIM-1) and low (below 7 T, NIM-2) working magnetic flux density were fabricated and characterized. The two devices were compared with the LEP-made device (BIPM-2) by calibrating the same NML 1 Ω standard resistor. The relative differences between the two calibrated values given by NIM-1 and BIPM-2, and NIM-2 and BIPM-2, are −0.69 parts in 10^9 and 2.5 parts in 10^9 respectively. The calibration results show that NIM-made devices can be used as standard devices for the quantum Hall resistance standard system.

Acknowledgments

The authors would like to thank Liu Yong for technical support during the CCC calibration measurements, and Fu Kai, Shi Yong, Wang Zezhang and Li Zhun for support on the low temperature measurements. This work was supported by the National Key Technology R&D Program (2011BAK15B08).

References

[1] von Klitzing K 1986 The quantized Hall effect *Rev. Mod. Phys.* **58** 519–31

[2] Van der Wel W, Haanappel E G, Mooij J E, Harmans C, Andr E J P, Weimann G, Ploog K, Foxon C T and Harris J J 1989 Selection criteria for AlGaAs-GaAs heterostructures in view of their use as a quantum Hall resistance standard *J. Appl. Phys.* **65** 3487–97

[3] Hartland A 1992 The quantum Hall effect and resistance standards *Metrologia* **29** 175–90

[4] Inglis A D and Minowa I 1997 Fabrication of precision quantized Hall devices *IEEE Trans. Instrum. Meas.* **46** 281–4

[5] Delahaye F, Witt T J, Pesel E, Schumacher B and Warnecke P 1997 Comparison of quantum Hall effect resistance standards of the PTB and the BIPM *Metrologia* **34** 211–4

[6] Delahaye F and Jeckelmann B 2003 Revised technical guidelines for reliable dc measurements of the quantized Hall resistance *Metrologia* **40** 217–23

[7] Jeckelmann B and Jeanneret B 2001 The quantum Hall effect as an electrical resistance standard *Rep. Prog. Phys.* **64** 1603–55

[8] Pierz K, Gotz M, Pesel E, Ahlers F and Schumacher H W 2011 Quantum Hall resistance standards with good quantization at high electron mobilities *IEEE Trans. Instrum. Meas.* **60** 2455–61

[9] Schopfer F and Poirier W 2013 Quantum resistance standard accuracy close to the zero-dissipation state *J. Appl. Phys.* **114** 064508

[10] Ahlers F J, Pierz K and Götz M 2016 Direct comparison of fractional and integer quantized Hall resistances: Status and perspectives *Conf. on Precision Electromagnetic Measurements (CPEM 2016)* pp 1–2

[11] Piquemal F, Geneves G, Delahaye F, Andre J, Patillon J and Frijlink P 1993 Report on a joint BIPM-EUROMET project for the fabrication of QHE samples by the LEP *IEEE Trans. Instrum. Meas.* **42** 264–8

[12] Zhang Z H, He Q, Li Z K and Liu Y G 2005 A study on the national standard of quantum Hall resistance *Acta Metrol. Sin.* **26** 97–101 (In Chinese)

[13] Zhong Y, Li J J, Zhong Q, Lu Y F, Zhao J T and Wang X S 2012 GaAs/AlGaAs quantum Hall resistance devices with AuGeNi and In contacts *Conf. on Precision Electromagnetic Measurements (CPEM)* pp 386–7

[14] Zhong Q, Li J J, Zhao J T, Zhao M K, Wang X S, Lu Y G and Zhong Y 2014 Investigation of single quantum Hall device of resistance standard in NIM *Conf. on Precision Electromagnetic Measurements (CPEM 2014)* pp 544–5

[15] Wang X S, Zhong Q, Li J J, Lu Y G, Zhong Y, Zhao M K, Li Z K and Li Z 2016 Development of single quantum Hall devices for the resistance standard in NIM *Conf. on Precision Electromagnetic Measurements (CPEM 2016)* pp 1–2

[16] Pierz K and Schumacher B 1999 Fabrication of quantum Hall devices for low magnetic fields *IEEE Trans. Instrum. Meas.* **48** 293–5

[17] Jeckelmann B and Jeanneret B 1997 Influence of the voltage contacts on the four-terminal quantized Hall resistance in the nonlinear regime *IEEE Trans. Instrum. Meas.* **46** 276–80

[18] Jeckelmann B, Rufenacht A, Jeanneret B, Overney F, Pierz K, von Campenhausen A and Hein G 2001 Optimization of QHE-devices for metrological applications *IEEE Trans. Instrum. Meas.* **50** 218–22

[19] He Q, Zhang Z H, Li Z K and Zhao J T 2008 Uncertainty budget for the NIM QHR standard system *Conf. on Precision Electromagnetic Measurements (CPEM 2008)* pp 160–1